THE JOURNAL OF BIOLOGICAL CHEMISTRY VOL. 281, NO. 24, pp. 16576–16582, June 16, 2006

Mutagenesis and Molecular Modeling Reveal the Importance of the 5-HT_3 Receptor F-loop*

Received for publication, February 9, 2006, and in revised form, March 29, 2006 Published, JBC Papers in Press, April 4, 2006, DOI 10.1074/jbc.M601265200

Andrew J. Thompson[‡], **Claire L. Padgett**[‡], **and Sarah C. R. Lummis**[‡§1]

From the [‡]*Department of Biochemistry, University of Cambridge, and the* [§]*Neurobiology Division, Laboratory of Molecular Biology, Cambridge, United Kingdom*

The 5-HT_3 receptor is a member of the Cys-loop family of ligand-gated ion channels. The extracellular domains of these proteins contain six amino acid loops (A–F) that converge to form the ligand binding site. In this study we have mutated 21 residues in or close to the 5-HT_3 receptor F-loop (Ile^{192} to Gly^{212}) to Ala or to a residue with similar chemical properties. Mutant receptors were expressed in HEK293 cells, and binding affinity was measured using [^{3}H]granisetron. Two regions displayed decreases in binding affinity when mutated to Ala (Ile^{192}–Arg^{196} and Asp^{204}–Ser^{206}), but only one region was sensitive when mutated to chemically similar residues (Ile^{192}–Val^{201}). Homology modeling using acetylcholine-binding protein crystal structures with a variety of different bound ligands suggests there may be distinct movements of Trp^{195} and Asp^{204} upon ligand binding, indicating that these residues and their immediate neighbors have the ability to interact differently with different ligands. The models suggest predominantly lateral movement around Asp^{204} and rotational movement around Trp^{195}, indicating the former is in a more flexible region. Overall our results are consistent with a flexible 5-HT_3 receptor F-loop with two regions that have specific but distinct roles in ligand binding.

The 5-HT_3[2] receptor is a transmembrane protein that is involved in signal transmission in the central and peripheral nervous systems. It is a member of the Cys-loop family of ligand-gated ion channels that also includes the nicotinic acetylcholine (nACh), zinc-activated, glycine, $GABA_A$ and $GABA_C$ receptors. The functional receptors consist of five symmetrically arranged subunits that surround a centrally located ion-conducting pore. Each subunit has a large extracellular N-terminal domain, four transmembrane domains (M1–M4), and a large intracellular loop between M3 and M4. The ligand binding site is located in the extracellular domain and is formed at the interface of two adjacent subunits (1–4). In the 5-HT_3 receptor, five subunits (A–E) have been identified, although only homomeric 5-HT_{3A} or heteromeric 5-$HT_{3A/B}$ subunit complexes have been functionally expressed and characterized (5, 6). Current evidence suggests 5-HT_3 receptors in the brain may be predominantly homomeric receptors, whereas in the peripheral nervous system heteromeric receptors may predominate (7).

Biochemical studies have identified a number of key residues involved in binding and have shown that the amino acids responsible for the receptor-ligand interaction are located in six convergent loops (A–F). In addition, structural insight has been gained from cryoelectron microscopy of the nACh receptor and from the crystal structures of the acetylcholine binding protein (AChBP), a soluble protein that is homologous to the extracellular region of Cys-loop receptors (8–11).

However, there are some important structural and functional differences between AChBP and Cys-loop receptors. For example, AChBP lacks a channel and shows little cooperativity in ligand binding, and it is not clear whether AChBP best resembles an activated, resting, or desensitized state of the nACh receptor (9).

Celie *et al.* (10) have used isothermal titration calorimetry to compare binding in AChBP from *Limnea. stagnalis* and *Bulinus truncatus* and found that residues in loops A–E could not account for differences in ligand binding affinity between the two proteins. This suggests that differences in binding in these, and in other related proteins, may be due to differences in their F loops, whose crystal structure is poorly resolved in all of the AChBP structures to date, and whose sequence is poorly conserved both between subunits of the same receptor type and between different members of the same Cys-loop family (1–4, 8, 9). This region is known to have a significant impact on ligand binding and may interact with ligands as they enter or exit the binding site (12–14). To date, only the $GABA_A$ α1 and $GABA_C$ ρ1 subunits have received a comprehensive study of the residues in the F-loop region, but due to the high levels of sequence variability in this region it is difficult to make comparisons between homologous residues across the Cys-loop family (13, 15). To gain a better understanding of the role of the F-loop in ligand binding in the 5-HT_3 receptor, we have mutated 21 consecutive amino acids in this region (Ile^{192} to Gly^{212}) and created a series of structural models of this region using a variety of AChBP crystal structures. Our results demonstrate the importance of the 5-HT_3 receptor F-loop region in ligand binding.

EXPERIMENTAL PROCEDURES

Materials—All cell culture reagents were obtained from Invitrogen, except fetal calf serum, which was from Labtech International (Ringmer, UK). [^{3}H]Granisetron (63.5 Ci/mmol) was from PerkinElmer Life Sciences. All other reagents were of the highest obtainable grade.

Cell Culture—Human embryonic kidney (HEK) 293 cells were maintained on 90-mm tissue culture plates at 37 °C and 7% CO_2 in a humidified atmosphere. They were cultured in Dulbecco's modified Eagle's medium/Nutrient Mix F12 (1:1) with GlutaMAX™ I media containing 10% fetal calf serum and passaged when confluent. For radioligand binding studies, cells in 90-mm dishes were transfected using calcium phosphate precipitation at 80–90% confluency and incubated for 3–4 days before use (16, 17). For functional studies cells were transfected by electroporation using the AMAXA system (Amaxa GmbH, Cologne, Germany), plated on 96-well plates, and incubated 1–2 days before assay.

* This work was supported by the Wellcome Trust, the Biotechnology and Biological Sciences Research Council, and Merck Sharp and Dohme. The costs of publication of this article were defrayed in part by the payment of page charges. This article must therefore be hereby marked "*advertisement*" in accordance with 18 U.S.C. Section 1734 solely to indicate this fact.

[1] A Wellcome Trust Senior Research Fellow in Basic Biomedical Studies. To whom correspondence should be addressed: Dept. of Biochemistry, University of Cambridge, Cambridge CB2 1QW, United Kingdom. Tel.: 44-1223-765-950; Fax: 44-1223-333-345; E-mail: sl120@cam.ac.uk.

[2] The abbreviations used are: 5-HT, 5-hydroxytryptamine; LGIC; ligand-gated ion channel; ACh, acetylcholine; AChBP, acetylcholine-binding protein; nACh, nicotinic acetylcholine; TBS, Tris-buffered saline; GABA, γ-aminobutyric acid.

Site-directed Mutagenesis—Mutagenesis reactions were performed using the method described by Kunkel (18). The 5-HT$_{3A}$ subunit DNA (accession: AY605711) has been described previously (19). Oligonucleotide primers were designed according to the recommendations of Sambrook *et al.* (20) and some suggestions of the Primer Generator (Ref. 21; www.med.jhu.edu/medcenter/primer/primer.cgi). A silent restriction site was incorporated into each primer to assist rapid identification.

Radioligand Binding—This was undertaken as previously described (22) with minor modifications. Briefly, transfected HEK293 cells were washed twice with phosphate buffered saline and then scraped into 1 ml of ice-cold HEPES buffer (10 mM, pH 7.4) containing the following proteinase inhibitors: 1 mM EDTA, 50 μg/ml soybean trypsin inhibitor, 50 μg/ml bacitracin, and 0.1 mM phenylmethylsulfonyl fluoride, and frozen at −20 °C. After thawing, they were washed twice with HEPES buffer, resuspended, and 50 μg of cell membranes was incubated in 0.5 ml of HEPES buffer containing the 5-HT$_3$ receptor antagonist [^{3}H]granisetron. Saturation binding (eight point) assays were performed on at least three separate plates of transfected cells for each mutant using 0.1–40 nM [^{3}H]granisetron. Nonspecific binding, determined using 1 μM quipazine, was routinely 5–10% of total binding. Reactions were incubated for 1 h at 4 °C and terminated by rapid vacuum filtration using a Brandel cell harvester onto GF/B filters pre-soaked in 0.3% polyethyleneimine followed by two rapid washes with 4 ml of ice-cold HEPES buffer. Radioactivity was determined by scintillation counting (Beckman LS6000sc). Protein concentration was estimated using the Bio-Rad Protein Assay with bovine serum albumin standards. Data were analyzed by iterative curve fitting (Prism, GraphPad Software, San Diego, CA) according to the equation, $B = (B_{max}\cdot[L])/(K + [L])$, where B is bound radioligand, B_{max} is maximum binding at equilibrium, K is the equilibrium dissociation constant, $[L]$ is the free concentration of radioligand. Values are presented as mean ± S.E. Statistical analysis was performed using analysis of variance in conjunction with Dunnett's post test.

Immunofluorescence—This was as described previously (23). Briefly, transfected cells were washed with three changes of Tris-buffered saline (TBS: 0.1 M Tris, pH 7.4, 0.9% NaCl) and fixed using ice-cold 4% paraformaldehyde in phosphate buffer (PB, 66 mM Na_2HPO_4, 38 mM NaH_2PO_4, pH 7.2). After two TBS washes, cells were incubated overnight at 4 °C in pAb120 at 1:1600 in TBS. Biotinylated anti-rabbit IgG (Vector Laboratories, Burlingame, CA) and fluorescein isothiocyanate avidin D (Vector) were used to detect bound antibody as per the manufacturer's instructions. Coverslips were mounted in Vectashield mounting medium (Vector). Immunofluorescence was observed using an Ultra*VIEW*^{TM} LCI Confocal Imaging System (PerkinElmer Life Sciences).

FLEXstation^{TM} Analysis—This was as previously described (24). Briefly, cells were gently rinsed twice with buffer (10 mM HEPES, 115 mM NaCl, 1 mM KCl, 1 mM $CaCl_2$, 1 mM $MgCl_2$, 10 mM glucose, pH 7.4). To each well 50 μl of buffer and 50 μl of fluorescent membrane potential dye (diluted 2:5 in buffer) were added, and the cells were incubated at room temperature for 45 min before assay. Fluorescence was measured in a FLEXstation^{TM} (Molecular Devices Ltd., Wokingham, UK) every 2 s for 200 s using the acquisition software SOFTmax® PRO version 4.3. Control (buffer alone) or 5-HT (0.001–30 μM) was added to each well at 20 s. Data were analyzed by iterative curve fitting using Prism version 4.03 (GraphPad Software) according to the equation, $F = F_{min} + ((F_{max} - F_{min})/1 + 10^{((\log EC_{50} - \log [L])nH)})$, where F_{min} is the baseline fluorescence at 20 s, F_{max} is the maximal fluorescence, EC_{50} is the concentration required for a half-maximal response, $[L]$ is the concentration of ligand, and nH is the Hill coefficient. Data are reported as means ± S.E. Statistical analysis was performed using Student's t test.

Modeling—This was performed as described previously (12, 25). Briefly, the three-dimensional models of the extracellular region of the 5-HT$_3$ receptor were built using MODELLER 6v2 (26) based on the crystal structure of AChBP in the unbound, agonist-bound, and antagonist-bound states (PDB codes: 2byn, 1uv6, 2byq, 1yi5, and 2byr). The pentamer was generated by superimposing the 5-HT$_3$ subunit on to each protomer of AChBP, with care taken not to alter the coordinate axes of reference. The generated pentameric model was energy minimized in SYBYL version 6.8 using the AMBER force field by moving side chains alone, to relieve short contacts at the inter-protomer interfaces (27). Electrostatic terms were included in these minimization cycles.

RESULTS

Effects of Mutations—Each amino acid along a sequence of 21 residues was mutated to either Ala or an amino acid with properties similar to the wild-type amino acid (subsequently referred to as a conserved amino acid change). The position of these residues within the linear sequence of the 5-HT$_3$ receptor is shown in Fig. 1 and is compared with AChBP and other Cys-loop receptors in Fig. 2.

The [^{3}H]granisetron binding affinity of the mutants is shown in Tables 1 and 2. Changing 10 of the 21 residues resulted in no significant change in affinity for either the Ala or conserved mutation, suggesting these residues do not play a role in ligand binding (Ser^{197}, Glu^{199}, Arg^{202}, Ser^{203}, Ile^{207}, Phe^{208}, Ile^{209}, Asn^{210}, Gln^{211}, and Gly^{212}). For the remaining 11 residues there were differences in binding affinities compared with wild type for one or both of the substitutions, suggesting that these residues have some role in [^{3}H]granisetron binding. These residues were Ile^{192}, Thr^{193}, Leu^{194}, Trp^{195}, Arg^{196}, Pro^{198}, Glu^{200}, Val^{201}, Asp^{204}, Lys^{205}, and Ser^{206}.

Effects of Alanine Mutations—Amino acid substitutions to Ala revealed significant changes in the [^{3}H]granisetron binding affinity for 8 of the 21 residues (Table 1). These changes were clustered into two groups at the N and C termini of the linear sequence. The changes to the N-terminal cluster extended from Ile^{192}, which lies immediately adjacent to the B-loop, through to Arg^{196}. From Ser^{197} to Ser^{203} all of the substitutions displayed a [^{3}H]granisetron binding affinity similar to wild type. The C-terminal cluster was Asp^{204}, Lys^{205}, and Ser^{206}. D204A displayed no specific binding at the concentrations of [^{3}H]granisetron used in this study. Immunofluorescence confirmed that this mutant was expressed at the cell surface, indicating that the mutation did not impair receptor assembly or membrane trafficking (Fig. 3). Binding was similar to wild type for Ala mutations from Ile^{207} through to Gly^{212}.

Effects of Conserved Mutations—Amino acid substitutions to residues with conserved properties revealed changes in the [^{3}H]granisetron binding affinity for 6 of the 21 residues (Table 2). The N-terminal cluster of residues, centered around Trp^{195}, that was sensitive to Ala mutation remained sensitive to conserved mutations and was extended to also include Pro^{198}, Glu^{200}, and Val^{201}. The C-terminal cluster displayed different properties to the Ala mutants, as conserved mutations at Asp^{204}, Lys^{205}, and Ser^{206} revealed wild-type binding affinities.

Functional Studies—To explore the role of Asp^{204} and Trp^{195} in agonist binding, 5-HT-induced responses in receptors with substitutions at these positions were examined using FLEXstation^{TM} analysis. This technique utilizes fluorescent voltage-sensitive dyes to detect changes in the membrane potential (24). The EC_{50} for 5-HT on wild-type receptors was 0.27 ± 0.06 μM ($n = 4$). Values from D204E mutant receptors were not significantly different to wild type (0.33 ± 0.09 μM, $n = 4$, $p <$ 0.05), whereas D204A mutant receptors were non-functional up to a

A

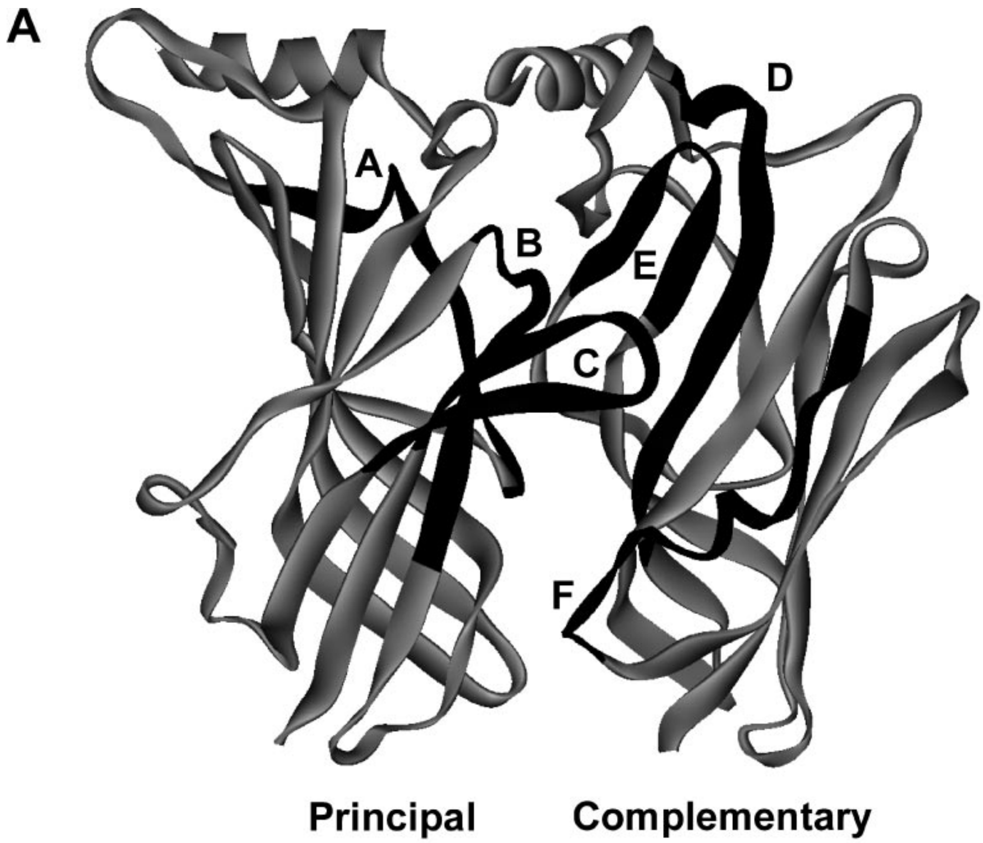

B

```
                          Loop D                       Loop A
5-HT3A  SMLTAPGEGSRRRATQEDTTQPALLRLSDHLLANYKKGVRPVRDWRKPTTVSIDVIMYAI   75
AChBP   ---MRRNIFCLACLWIVQACLSLDRADILYNIRQTSRPDVIPTQRDRPVAVSVSLKFINI   38
                                                        β1

5-HT3A  LNVDEKNQVLTTYIWYRQYWTDEFLQWTPEDFDNVTKLSIPTDSIWVPDILINEFVDVGK  135
AChBP   LEVNEITNEVDVVFWQQTTWSDRTLAWNSSH--SPDQVSVPISSLWVPDLAAYNAISKP-   95
                  β2                        β3          β4

            Loop E                                  Loop B
5-HT3A  SP-NIPYVYVHHRGEVQNYKPLQLVTACSLDIYNFPFDVQNCSLTFTSWLHTIQDINITL  194
AChBP   EVLTPQLARVVSDGEVLYMPSIRQRFSCDVSGVDTESG-ATCRIKIGSWTHHS--REI--  150
        β5      β5′     β6      β6′                  β7

                Loop F                    Loop C
5-HT3A  W-RSPEEVRSDKSIFINQ-GEWELLEVFPQFKEFS-IDISNSYAEMKFYVIIRRRPLFYAV  252
AChBP   -SVDPTTENSDDSEYFSQYSRFEILDVTQKKNSVTYSCCPEAYEDVEVSLNFRKKGRSEIL  210
         β8                         β9                  β10
```

FIGURE 1. **Location of the amino acid residues described in the current study.** *A*, two adjacent subunits (principal and complementary) showing the positions of the main binding loops. *B*, the amino acid sequence for the extracellular domain of the murine 5-HT$_{3A}$ receptor (accession number: Q6J1J7), aligned with AChBP isolated from *L. stagnalis* (accession number: P58154). The residues described in this study are highlighted as *white text* on a *black background*. The loops are indicated by *black lines* above the text. The positions of the β-sheets are shown by *gray lines* beneath the text. Numbering of residues and structural features are taken from the AChBP crystal structure (9).

```
                  Loop B           Loop F            Loop C
Snail AChBP       THHSREI----SVDPTTENSDDSEYFSQYSRFEILDVTQK    179
Mouse 5-HT3A      TIQDINITLW--RSPEEVRSDKSIFINQ-GEWELLEVFPQ    222
Rat GABAA α1      -TRAEVVYEW-TREPARSVVVAEDGSRL-NQYDLLGQTVD    225
Rat nACh γ        QEDGQAIE-WIFIDPEAFTENGEWAIRHRPAKMLL--DPV    220
Rat nACh δ        -DNRSYPIEWIIIDPEGFTENGEWEIVH-RAAKVNV-DPS    225
Rat nACh ε        VDDDGNAINKIDIDTAAFTENGEWAID-YCPGMIRHYEG-    219
Rat Gly α1        YTMNDLIFEWQEQGAVQVA-DGLTLPQ-FILKEEKDLRYC    226
```

FIGURE 2. **Alignment of the F-loop residues of members of the Cys-loop family of ligand-gated ion channels.** Accession numbers for the alignment are as follows: pond snail AChBP, P58154; mouse 5-HT$_{3A}$, Q6J1J7; rat GABA$_A$ α1, P62813; rat nACh γ, P18916; rat nACh δ, P25110; rat nACh ϵ, P09660; and rat glycine α1, P07727.

TABLE 1
Effects of Ala substitutions on [^{3}H]granisetron binding affinities to the 5-HT$_3$ receptor

Alanine Mutant	K_d (nM) Mean ± SEM	n	K_d (nM) 0 5 10 15 20
Wild Type	1.37 ± 0.22	19	
I192A[&]	8.00 ± 0.59	5	
T193A[&]	5.26 ± 0.96	10	
L194A[&]	10.7 ± 1.50	5	
W195A[&]	11.8 ± 1.47	6	
R196A[&]	14.9 ± 2.94	4	
S197A	1.34 ± 0.10	5	
P198A	0.75 ± 0.61	5	
E199A	0.59 ± 0.10	6	
E200A	0.72 ± 0.10	6	
V201A	1.62 ± 0.10	3	
R202A	0.80 ± 0.09	3	
S203A	0.20 ± 0.05	3	
D204A[&]	NB	6	
K205A[&]	19.0 ± 1.88	4	
S206A[&]	4.37 + 0.35	7	
I207A	0.97 ± 0.08	3	
F208A	0.31 ± 0.03	3	
I209A	1.52 ± 0.17	6	
N210A	0.60 ± 0.07	6	
Q211A	1.16 ± 0.25	6	
G212A	1.02 ± 0.07	4	

[&] Significantly different from wild type (analysis of variance with Dunnett's post test: $p < 0.05$). NB, no binding.

TABLE 2
Effects of conserved amino acid changes on [^{3}H]granisetron binding affinities to the 5-HT$_3$ receptor

Conserved Mutant	K_d (nM) Mean ± SEM	n	K_d (nM) 0 5 10 15 20
Wild Type	1.37 ± 0.22	19	
I192L	2.67 ± 0.41	8	
T193S[&]	4.97 ± 0.74	6	
L194I	3.25 ± 0.52	6	
W195Y[&]	16.9 ± 2.68	5	
R196K[&]	5.96 ± 1.06	3	
S197T	4.26 ± 1.58	4	
P198H[&]	8.55 ± 1.86	5	
E199D	2.08 ± 0.45	6	
E200D[&]	5.13 ± 2.00	3	
V201L[&]	5.29 ± 0.93	7	
R202K	0.35 ± 0.10	3	
S203T	0.26 ± 0.11	3	
D204E	1.20 ± 0.32	3	
D204N	1.03 ± 0.17	6	
K205R	1.59 ± 0.11	6	
K205M	1.11 ± 0.20	3	
S206T	4.13 ± 0.35	6	
I207L	1.55 ± 0.12	5	
F208Y	2.33 ± 0.19	6	
I209L	2.08 ± 0.16	4	
N210Q	2.11 ± 0.45	4	
Q211N	2.53 + 0.30	4	
G212N	1.02 ± 0.07	4	

[&] Significantly different from wild type (analysis of variance with Dunnett's post test: $p < 0.05$).

5-HT concentration of 30 μM ($n = 8$). An increase of ~10-fold in the EC_{50} value for W195A receptors was significantly greater than wild-type receptors (3.3 ± 0.5 μM, $n = 4$, $p < 0.05$) and was similar to previously published increases for W195Y (4-fold increase) and W195S (9-fold increase) mutants (28).

F-loop Modeling—To gain further insight into the importance of the F-loop, a series of models were generated, based upon crystal structures of AChBP in different states; unbound (PDB ID: 2byn), agonist-bound

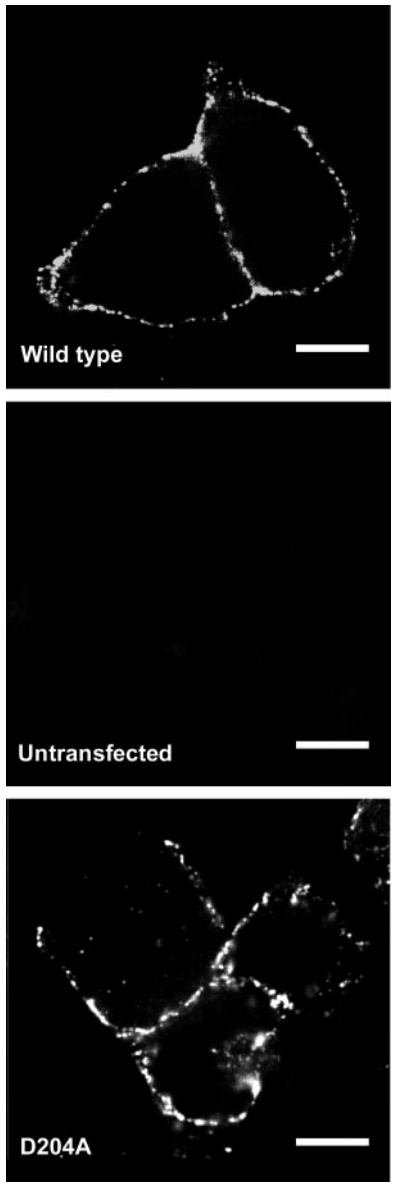

FIGURE 3. **Confocal images of immunofluorescent-labeled, non-permeabilized HEK293 cells.** Cell-surface expression of wild-type receptors (*A*). No fluorescence was visible in untransfected cells (*B*). Cells transfected with D204A displayed conspicuous fluorescence on the cell periphery, indicating receptors were expressed and had reached the cell surface (*C*). *Scale bar*, 12 μm.

(carbamylcholine, PDB ID: 1uv6 and epibatidine, PDB ID: 2byq), and antagonist-bound (2-methyllcaconitine, PDB ID: 2byr and α-cobratoxin, PDB ID: 1yi5) (8, 29, 30). The lowest energy state for each model is shown in Fig. 4. An overlay of the backbone carbons (Fig. 4*F*) for each of the models suggests that the F-loop does not undergo rigid body movements but displays conformational flexibility that is dependent upon the bound ligand. To demonstrate this point, the inter-subunit distances between the α-carbon of Trp^{183} (principal subunit) and the α-carbon of either Trp^{195} or Asp^{204} (complementary subunit) were calculated (Table 3). Trp^{183} was chosen as a reference point, because there is considerable evidence regarding the importance of this residue and it is known to be centrally located within the binding pocket (12, 25, 28, 31, 32). The distances between α-carbons of Trp^{183} residues of adjacent subunits were included as an internal control for widespread disruption of the whole binding site.

TABLE 3

Distances (Å) from the α-carbon of Trp^{183} in the principal subunit to the α-carbon of residues across the interface in the complementary subunit

Thr^{64} and Ser^{66} are shown below to demonstrate their proximity to Trp^{195}.

	Distance from Trp183 to the adjacent subunit residue (Å)		
	Trp-183 to Trp-183	*Trp-183 to Trp195*	*Trp-183 to Asp-204*
Unbound [a]	26.66	23.93	16.53
Agonist [b]	26.65	24.00	19.05
Agonist [c]	26.20	24.39	18.35
Large Antagonist [d]	27.30	25.56	22.49
Small Antagonist [e]	27.07	26.11	16.78

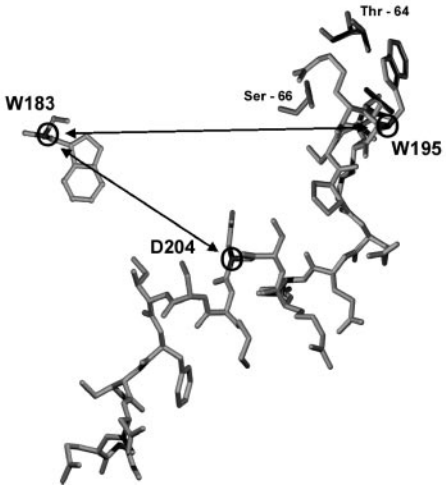

[a] Modeled from AChBP with no ligand bound (PDB ID: 2byn).
[b] AChBP with carbamylcholine (PDB ID: 1uv6).
[c] AChBP with epibatidine (PDB ID: 2byq).
[d] AChBP with α-cobratoxin (PDB ID: 1yi5).
[e] AChBP with 2-methyllycaconitine (PDB ID: 2byr).

Comparison of the Trp^{183} to Trp^{183} distances for each of the models revealed that these are similar (26.20–27.07 Å) and indicates that any variability in the measurements of Trp^{195} and Asp^{204} is unlikely to be the result of macroscopic disruptions of the binding pocket region. Lateral movements of the Trp^{195} α-carbon positions are small across the range of models, but there are significant rotational movements (Fig. 4, *A*–*E*). These are most pronounced for the antagonist-bound models, which show that the side chain of Trp^{195} rotates clockwise from a 12 o'clock position to a three or six o'clock positions (Fig. 4, *E* and *D*). Distances between the α-carbon of Asp^{204} and the α-carbon of Trp^{183} in both the agonist-bound structures are greater than in the unbound form, suggesting that there is movement in this region during binding (Table 3). In contrast, binding of the small antagonist does not cause lateral movement, although the greatest movement of Asp^{204} is seen upon binding of the large antagonist, which causes Asp^{204} to move away from Trp^{183} and toward the solvent.

DISCUSSION

This study describes the affects of substitutions across a 21-amino acid stretch that incorporates the 5-HT$_3$ receptor F-loop. Residues were mutated to either Ala or to an amino acid with chemical properties similar to the wild-type residue. Mutation of 11 of the amino acids caused changes in the binding affinity of [^{3}H]granisetron, suggesting that they have a role here. The data revealed two clusters of residues of particular importance, centered around Trp^{195} and Asp^{204}. Modeling, based upon the structures of AChBP bound to a variety of ligands, supports the hypothesis that the F-loop forms a flexible structure and suggests that upon ligand binding there are specific, but distinct movements of Trp^{195} and Asp^{204}.

Trp^{195} has previously been identified as a potentially important binding residue in the 5-HT$_3$ receptor: both EC$_{50}$ values for 5-HT and K_d values for [^{3}H]granisetron were substantially increased when Trp^{195} was mutated to Tyr or Ser, similar to the observations presented here (28). As proposed in the previous study, our results support a role for this residue in binding rather than gating, and indeed it may contribute to the aromatic box that is critical for all Cys-loop receptors. Because Trp^{195} is important, changes in binding affinity observed when mutating the neighboring amino acids may reflect indirect effects resulting from their proximity to Trp^{195}. However, it is more likely, given the range of residues that cause a change in binding affinity when mutated (Ile^{192}–Val^{201}), that other residues in this region also contribute to ligand binding, either directly or via contributions to the structure of the binding site. Our homology models show Trp^{195} and Arg^{196} are in close association with residues from other regions of the protein, and therefore may be involved in interactions that permit the correct folding of the binding pocket. For example, Trp^{195} is <5 Å from Thr^{64} and Ser^{66} with which it might hydrogen bond (Table 3). Perhaps surprisingly, the charged side chains of Glu^{199} and Arg^{202} do not appear to be important, because both Ala and conserved substitutions do not significantly alter the binding affinity in these mutant receptors. Even an Ala substitution at Pro^{198} was well tolerated, which was unexpected as studies have shown that a number of 5-HT$_3$ receptor Pro residues are critical for binding and/or function (33). There is not an ideal conservative substitution for proline, although changing it to His (which also has a 5-membered ring but is slightly larger) did cause an increase in K_d, indicating that size may be important here. Size may also play a role at Glu^{200} and Val^{201}, where a change in binding affinity was observed with conservative but not Ala substitutions.

The second cluster of amino acids consists of Asp^{204}, Lys^{205}, and Ser^{206}. D204A was the only Ala mutation in the F-loop that completely ablated binding, indicating the importance of this residue. No functional response was observed with this mutant receptor, although immunofluorescence showed it was capable of reaching the cell surface. This is consistent with the lack of function being due solely to the lack of binding. Interestingly, Asp^{204} and Lys^{205} displayed wild-type binding affinities when their positive charges were preserved in the conserved mutations, suggesting the formation of salt-bridges. However, eliminating the charge in the D204N and K205M mutants showed that is not the case. The amino acids aligning with Asp^{204} in the GABA$_A$ α subunit (Val^{180}) and nACh receptor γ (Asp^{203}), δ (Asp^{208}), and ε (Asp^{202}) subunits have all been implicated in ligand binding, and the Lys^{205} equivalent (Ala^{181}) in GABA$_A$ receptor α subunits has also been shown to be important (4, 13, 34–36). Therefore, it is likely that this region contributes to ligand binding in all Cys-loop receptors.

Despite the lack of structural information, there is evidence from the GABA$_A$ receptor that the F-loop may undergo a structural re-arrangement upon ligand binding (13). Using pentobarbital (which activates the channel at a site remote from the ligand binding site), methanethiosulfonate ethylammonium modification of cysteine mutants indicated that Val^{180} (which aligns with Asp^{204} in the 5-HT$_3$ receptor), Ala^{181} (Lys^{205}), and Arg^{186} (Asn^{210}) undergo structural changes during ligand binding and/or channel opening. It was also noted that Val^{178} (Arg^{202}), Val^{180} (Asp^{204}), and Asp^{183} (Ile^{207}) are likely to contribute to the receptor binding site. Our homology modeling suggests that there is also movement in the 5-HT$_3$ receptor F-loop region, around the two clusters of residues that were identified as important in our mutagenesis studies. Our data indicate rotational movement in the region of Trp^{195} and both lateral and rotational movement around Asp^{204}. Trp^{195} is located immediately

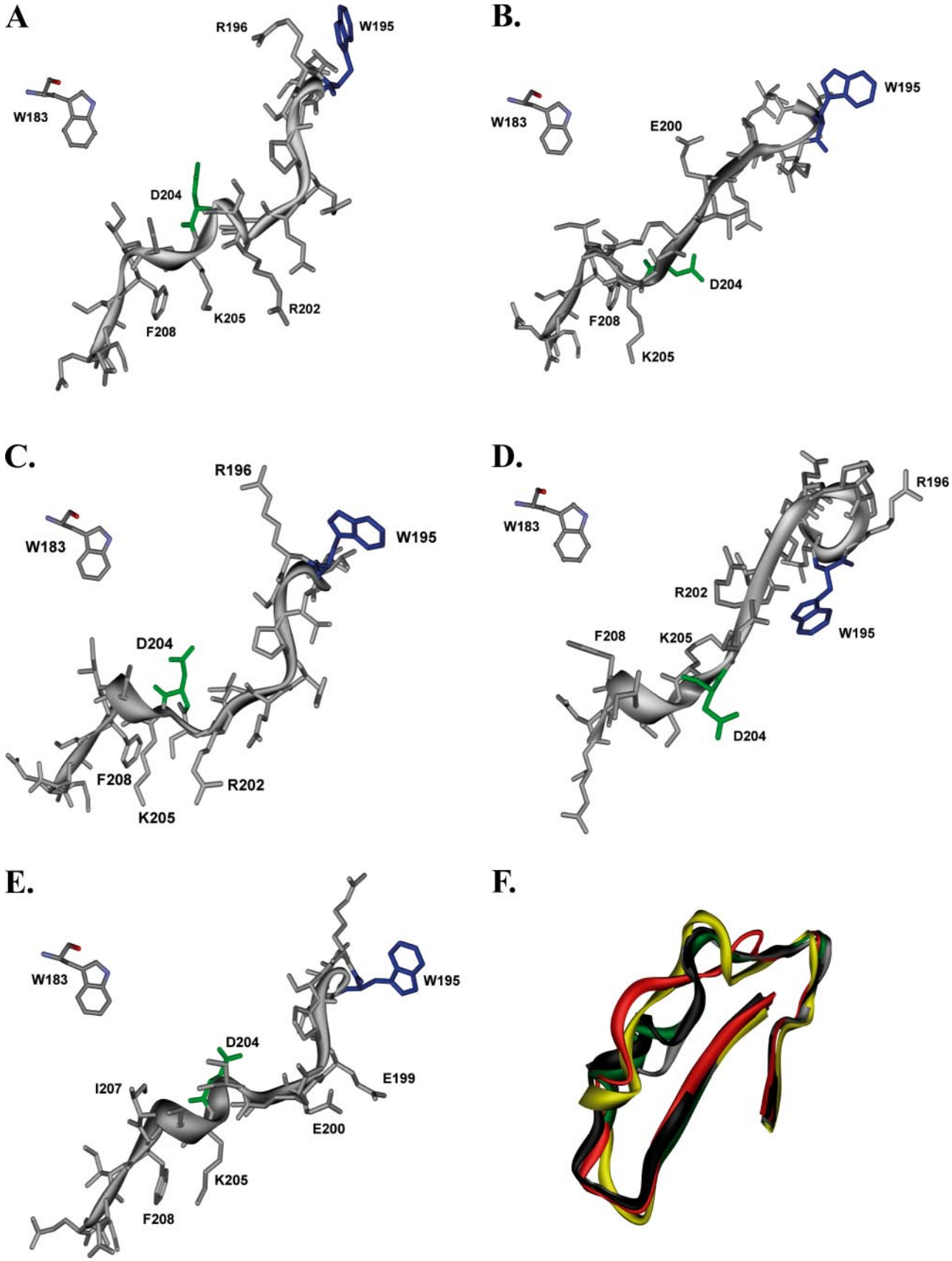

FIGURE 4. **Five modeled F-loops showing Trp^{183} for orientation.** *A*, unbound structure (modeled from AChBP with no ligand, PDB ID: 2byn). *B*, agonist-bound (AChBP with carbamylcholine, PDB ID: 1uv6). *C*, agonist-bound (AChBP with epibatidine, PDB ID: 2byq). *D*, large antagonist-bound (AChBP with α-cobratoxin, PDB ID: 1yi5). *E*, small antagonist-bound, (AChBP with 2-methyllycaconitine, PDB ID: 2byr). *F*, relative positions of the modeled F-loops as compiled by Swiss-PdbViewer "magic fit," using the adjacent β8 and β9 sheets as reference points (A, *black*; B, *red*; C, *gray*; D, *yellow*; and E, *green*).

downstream of the β8-sheet, and lateral movement here may be limited by the anchoring effect of this rigid β-sheet structure. Interactions between this β-sheet and the region around Trp^{195} could be important, because the adjacent β9 and β10 strands are part of the C-loop. Therefore, movement around Trp^{195} could directly affect the C-loop and have an impact on ligand binding or subsequent receptor movement. More structural information, especially comparisons of the closed and open states of the receptor, is needed to support this hypothesis. It is also noteworthy that in some studies researchers have subdivided the F-loop (*e.g.* Ref. 37). Our data would support the idea that there is more than one important region in this loop, but given the structural evidence from AChBP it seems logical to consider the region as a whole until further evidence suggests otherwise.

Comparisons of AChBP and nACh receptor structure indicate that conformational changes in the binding site are predominantly within the C- and F-loop regions. The C-loop is proposed to undergo a rigid body movement that changes its position from one that is extended toward the solvent when in the resting state, to one that contracts around the ligand in the agonist-bound conformation (8, 10, 30). In contrast, there is strong evidence that the F-loop is flexible, and in many of the crystallization studies of AChBP the F-loop is poorly resolved due to its unordered structure (9, 10). Where we do have structural information, comparisons of the F-loop in AChBP from different species has revealed a high level of variability, supporting the hypothesis that the F-loop may play a role in subunit specific pharmacological characteristics (13, 38, 39).

Our models show that there are significant differences in the orientation and positioning of the residues Trp^{195} and Asp^{204} that depend upon the ligand but not necessarily on whether the ligand is an agonist or antagonist. The distance of Asp^{204} from Trp^{183} (located in the center of the binding site) was similar in both the unbound and small antagonist-bound models, consistent with thinking that antagonists lock the receptor in the resting state. However, the presence of a large antagonist appeared to cause a large lateral displacement of Asp^{204} away from Trp^{183} (5.96 Å), providing some support for the recent proposal that large antagonists push the components of the binding pocket further apart (30). The change in the position of Trp^{195} was smaller for both small and large antagonists (2.18 and 1.63 Å). Agonists, on the other hand, appear to cause very little displacement of Trp^{195} (<0.5 Å) but do appear to displace Asp^{204}; in the two agonist-bound models Asp^{204} is 1.82 and 2.52 Å further away from Trp^{183} than in the unbound state. These movements may not only contribute to conformational changes within the F-loop but may also influence other closely located binding loops, such as the adjacent β9 and β10 region of the C-loop.

In summary, we have shown that residues within the F-loop region, and in particular those centered around Trp^{195} and Asp^{204}, are critical for antagonist binding in the 5-HT$_3$ receptor. Combining these data with our modeling studies suggests F-loop residues are important contributors to the binding of all ligands and also have the potential to cause or influence conformational changes in or close to the binding pocket. Such changes may be common to all Cys-loop receptors.

REFERENCES

1. Corringer, P. J., Le Novere, N., and Changeux, J. P. (2000) *Annu. Rev. Pharmacol. Toxicol.* **40,** 431–458
2. Akabas, M. H. (2004) *Int. Rev. Neurobiol.* **62,** 1–43
3. Reeves, D. C., and Lummis, S. C. (2002) *Mol. Membr. Biol.* **19,** 11–26
4. Sine, S. M. (2002) *J. Neurobiol.* **53,** 431–446
5. Davies, P. A., Pistis, M., Hanna, M. C., Peters, J. A., Lambert, J. J., Hales, T. G., and Kirkness, E. F. (1999) *Nature* **397,** 359–363
6. Niesler, B., Frank, B., Kapeller, J., and Rappold, G. A. (2003) *Gene* **310,** 101–111
7. Morales, M., and Wang, S. D. (2002) *J. Neurosci.* **22,** 6732–6741
8. Celie, P. H., van Rossum-Fikkert, S. E., van Dijk, W. J., Brejc, K., Smit, A. B., and Sixma, T. K. (2004) *Neuron* **41,** 907–914
9. Brejc, K., van Dijk, W. J., Klaassen, R. V., Schuurmans, M., van Der Oost, J., Smit, A. B., and Sixma, T. K. (2001) *Nature* **411,** 269–276
10. Celie, P. H., Klaassen, R. V., van Rossum-Fikkert, S. E., van Elk, R., van Nierop, P., Smit, A. B., and Sixma, T. K. (2005) *J. Biol. Chem.* **280,** 26457–26466
11. Unwin, N. (2005) *J. Mol. Biol.* **346,** 967–989
12. Thompson, A. J., Price, K. L., Reeves, D. C., Chan, S. L., Chau, P. L., and Lummis, S. C. (2005) *J. Biol. Chem.* **280,** 20476–20482
13. Newell, J. G., and Czajkowski, C. (2003) *J. Biol. Chem.* **278,** 13166–13172
14. Thompson, A. J., Chau, P. L., Chan, S. L., and Lummis, S. C. (2006) *Biophys. J.* **90,** 1979–1991
15. Sedelnikova, A., Smith, C. D., Zakharkin, S. O., Davis, D., Weiss, D. S., and Chang, Y. (2005) *J. Biol. Chem.* **280,** 1535–1542
16. Chen, C. A., and Okayama, H. (1988) *BioTechniques* **6,** 632–638
17. Jordan, M., Schallhorn, A., and Wurm, F. M. (1996) *Nucleic Acids Res.* **24,** 596–601
18. Kunkel, T. A. (1985) *Proc. Natl. Acad. Sci. U. S. A.* **82,** 488–492
19. Hargreaves, A. C., Lummis, S. C., and Taylor, C. W. (1994) *Mol. Pharmacol.* **46,** 1120–1128
20. Sambrook, J., Fritsch, E. F., and Maniatis, T. (1989) *Molecular Cloning: A Laboratory Manual*, 2nd Ed., Cold Spring Harbor Laboratory Press, Cold Spring Harbor, NY
21. Turchin, A., and Lawler, J. F., Jr. (1999) *BioTechniques* **26,** 672–676
22. Lummis, S. C., Sepulveda, M. I., Kilpatrick, G. J., and Baker, J. (1993) *Eur. J. Pharmacol.* **243,** 7–11
23. Spier, A. D., Wotherspoon, G., Nayak, S. V., Nichols, R. A., Priestley, J. V., and Lummis, S. C. R. (1999) *Mol. Brain Res.* **71,** 369
24. Price, K. L., and Lummis, S. C. (2005) *J. Neurosci. Methods* **149,** 172–177
25. Reeves, D. C., Sayed, M. F., Chau, P. L., Price, K. L., and Lummis, S. C. (2003) *Biophys. J.* **84,** 2338–2344
26. Sali, A., and Blundell, T. L. (1993) *J. Mol. Biol.* **234,** 779–815
27. Weiner, S. J., Kollman, P. A., Case, D. A., Singh, U. C., Ghio, C., Alagona, G., Profeta, S., and Weiner, P. (1984) *J. Am. Chem. Soc.* **106,** 765–784
28. Spier, A. D., and Lummis, S. C. (2000) *J. Biol. Chem.* **275,** 5620–5625
29. Bourne, Y., Talley, T. T., Hansen, S. B., Taylor, P., and Marchot, P. (2005) *EMBO J.* **24,** 1512–1522
30. Hansen, S. B., Sulzenbacher, G., Huxford, T., Marchot, P., Taylor, P., and Bourne, Y. (2005) *EMBO J.* **24,** 3635–3646
31. Beene, D. L., Brandt, G. S., Zhong, W., Zacharias, N. M., Lester, H. A., and Dougherty, D. A. (2002) *Biochemistry* **41,** 10262–10269
32. Zhong, W. G., Gallivan, J. P., Zhang, Y. O., Li, L. T., Lester, H. A., and Dougherty, D. A. (1998) *Proc. Natl. Acad. Sci. U. S. A.* **95,** 12088–12093
33. Deane, C. M., and Lummis, S. C. (2001) *J. Biol. Chem.* **276,** 37962–37966
34. Czajkowski, C., Kaufmann, C., and Karlin, A. (1993) *Proc. Natl. Acad. Sci. U. S. A.* **90,** 6285–6289
35. Martin, M., Czajkowski, C., and Karlin, A. (1996) *J. Biol. Chem.* **271,** 13497–13503
36. Czajkowski, C., and Karlin, A. (1995) *J. Biol. Chem.* **270,** 3160–3164
37. Arias, H. R. (2000) *Neurochem. Int.* **36,** 595–645
38. Ranna, M., Sinkkonen, S. T., Moykkynen, T., Uusi-Oukari, M., and Korpi, E. R. (2006) *BMC Pharmacol.* **6,** 1
39. Solt, K., Stevens, R. J., Davies, P. A., and Raines, D. E. (2005) *J. Pharmacol. Exp. Ther.* **316,** 771–776